FERMI LIQUID VISCOSITY IN A FINITE GEOMETRY

J.E. Jaffe

Laboratory of Atomic and Solid State Physics

Cornell University

Ithaca, New York 14853

ABSTRACT

Forced flow of a Fermi liquid is studied for a cell geometry consisting of two planes with a separation on the order of the mean free path. An approximate transport equation is used to derive an integral equation for the velocity profile, which is solved numerically. Results for the total flux through the cell, which determines the dissipation, are given as a function of the Knudsen number $\varkappa$ (ratio of cell thickness to mean free path.) Effects of specular reflection at the boundaries are considered. It is found that the dissipation has a minimum at $\varkappa \cong \frac{1}{2}$, and behaves linearly for $\varkappa \geq 3$. Implications for present experimentation are discussed.

FERMI LIQUID VISCOSITY IN A FINITE GEOMETRY

J.E. Jaffe

Laboratory of Atomic and Solid State Physics

Cornell University

Ithaca, New York 14853

ABSTRACT

Forced flow of a Fermi liquid is studied for a cell geometry consisting of two planes with a separation on the order of the mean free path. An approximate transport equation is used to derive an integral equation for the velocity profile, which is solved numerically. Results for the total flux through the cell, which determines the dissipation, are given as a function of the Knudsen number $\varkappa$ (ratio of cell thickness to mean free path.) Effects of specular reflection at the boundaries are considered. It is found that the dissipation has a minimum at $\varkappa \cong \frac{1}{2}$, and behaves linearly for $\varkappa \geq 3$. Implications for present experimentation are discussed.

I. Introduction

Recent experiments[1,2,3] have provided precise measurements of the transport properties of the various phases of ^{3}He to below 1 mK°. In this temperature regime the mean free path of the quasiparticles approaches or exceeds the dimensions of the experimental apparatus. This means that quasiparticles scattered from one boundary of the apparatus will not relax into local equilibrium with the rest of the fluid before they reach another boundary. The mean free path in the normal phase may approach 50 μm, and is much larger in the superfluid phases[4], while Andronikashvili cells presently in use have a thickness on the order of 100 μm. In consequence, the viscosity can no longer be related to measured quantities (e.g. drag forces) by the usual formulas of macroscopic fluid or superfluid mechanics. It is therefore necessary to understand such finite size effects in order to interpret present experiments.

This paper aims to shed some light on this problem by analyzing a particular case, namely Poisieulle flow, or forced flow of a normal fermi liquid between stationary infinite planes. We will calculate the total flux through the cell, which determines the rate of energy dissipation. In the large-cell limit this flux is inversely proportional to the viscosity, so the finite-cell flux may be taken to be inversely proportional to an "effective viscosity" that depends on the cell thickness. The ratio of this "effective viscosity" to the true viscosity of the bulk fluid conveniently characterizes the effect from an intuitive standpoint, although the dissipation is more closely related to the measured quantities. Some recent experiments[1,3] will be considered in the context of this theory, and possible relevance to future experiments discussed in the conclusion.

II. Choice of a Model

Consider a Fermi liquid flowing between stationary walls. The flow is sustained by a static, uniform force and is taken to be in the x-direction.

The cell is taken to be of infinite extent in the x- and y-directions and to extend from $z = -D/2$ to $z = D/2$. (See fig. 1) The system clearly has mirror symmetry in the xy-plane.

We will consider the quasiparticle transport equation for this system. The Landau interaction between quasiparticles[5] will be seen to cancel out of this equation, and enters the problem only through the quasiparticle lifetime τ[6]. We will treat the latter as a given quantity, since we are interested in the comparison of a finite and an infinite sample of the same fluid. If we treat particle-particle scattering in the same manner in both cases, the deficiencies of the relaxation time approximation should not drastically affect our basic results. We will see that τ contains the entire temperature as well as interaction dependence in the problem.

The simplest model which can be used for the scattering of particles from a wall is that of completely diffuse reflection. This means that the particles emerging from the wall after colliding with it possess a distribution which is isotropic in the reference frame of the wall and which corresponds to local equilibrium conditions at the point of collision. A more general model, which we shall use, is to assume that a fraction ε of the particles are specularly reflected[7], that is, the component of their momentum perpendicular to the wall is reversed and the other components are unchanged by scattering from the wall. This is certainly not the most general possible reflection process, but since very little is known about the quasiparticle-reflecting properties of experimental surfaces, it should be sufficient for our purposes. We consider ε as an adjustable parameter; we will see that the ε-dependence of our results can easily be separated from the other dependences.

III. Derivation of the Integral Equation

The number of quasiparticles per unit phase volume with momentum $\vec{p}$ at a height z in the cell is written $n_{\vec{p}}(z)$. In the absence of the applied force

field this becomes equal to the global equilibrium distribution function, which is written

$$n_{\vec{p}}^{0} = \frac{1}{e^{\beta(\varepsilon_p^0 - \mu)} + 1} \tag{1}$$

Here $\beta = 1/k_B T$, $\varepsilon_p^0 = p^2/2m^*$ where m^* is the effective mass, and μ is the chemical potential. We make the approximation that the temperature and chemical potential remain constant and uniform[8]. The average velocity of the fluid at height z, or "velocity profile", is given by

$$\vec{u}(z) = \sum_{\vec{p}} \vec{v}_{\vec{p}}\, n_{\vec{p}}(z) \quad ,$$

where $\vec{v}_{\vec{p}}$ is the velocity of a quasiparticle with momentum $\vec{p}$. Since the fluid flow is entirely in the x-direction, we may write

$$u(z) = \sum_{\vec{p}} \frac{p_x}{m^*} n_{\vec{p}}(z) \tag{2}$$

we also define

$$\delta n_{\vec{p}}(z) = n_{\vec{p}}(z) - n_{\vec{p}}^{0} \quad , \tag{3}$$

$$\varepsilon_{\vec{p}}(z) = \varepsilon_p^0 + \sum_{\vec{p}'} f_{\vec{p}\vec{p}'}\, \delta n_{\vec{p}'}(z) \quad ,$$

where $f_{\vec{p}\vec{p}'}$, is the Landau quasiparticle interaction function. We also define the local equilibrium distribution function and the deviation of the actual distribution from it:

$$n_p^{\ell e}(z) = \frac{1}{e^{\beta(\varepsilon_p(z)-p_x u(z)-\mu)}+1} \quad , \tag{5}$$

$$\delta\bar{n}_p(z) = n_p(z)-n_p^{\ell e}(z) \ . \tag{6}$$

We observe from (2), (5), and (6) that

$$\sum_p \vec{p}\delta\bar{n}_p(z) = 0 \ . \tag{7}$$

The transport equation is given by

$$\frac{\partial n_p}{\partial t}(z) + \vec{\nabla}_p \varepsilon_p \vec{\nabla}_r n_p(z) + \vec{F}_p(z)\cdot\vec{\nabla}_p n_p(z) = I[n_p'] \ , \tag{8}$$

where $I[n_p,]$ denotes the collision integral and the force $\vec{F}_p(z)$ on a quasi-particle with momentum $\vec{p}$ includes both the external field $\vec{F}$ and a mean field part:

$$\vec{F}_p(z) = \vec{F} - \vec{\nabla}_r \sum_{p'} f_{pp'} \delta n_{p'}(z) \ . \tag{9}$$

We now assume that the system is in a steady state, and approximate the collision integral by

$$I[n_p,] = -\frac{\delta\bar{n}_p(z)}{\tau} \ . \tag{10}$$

We also linearize in the quantities F, u, δn_p, $\delta\bar{n}_p$, and use the fact that $\vec{F}$ is in the x-direction while all spatial gradients are in the z-direction. We find that the term containing $f_{pp'}$, which comes from the third term on the left side of the transport equation (6) is cancelled by a similar term arising from the second term in (6). The transport equation becomes

$$\left(\frac{\partial}{\partial z} + \frac{m^*}{p_z\tau}\right)\delta\vec{n}_{\vec{p}}(z) = p_x\left(\frac{\partial u}{\partial z} - \frac{F}{p_z}\right)\left(\frac{\partial n_p^0}{\partial \varepsilon_p}\right) \quad . \tag{11}$$

This differential equation in z has the general solution

$$\delta\vec{n}_{\vec{p}}(z) = \exp(-m^*z/p_z\tau)\left\{A_{\vec{p}} + \int_{-D/z}^{z} dz' \exp(m^*z'/p_z\tau)p_x\left(\frac{\partial u}{\partial z}, - \frac{F}{p_z}\right)\left(\frac{\partial n_p^0}{\partial \varepsilon_p}\right)\right\} \tag{12}$$

where $A_{\vec{p}}$ is an arbitrary function of $\vec{p}$. When we apply boundary conditions to (12) we will obtain an explicit expression for $\delta n_{\vec{p}}(z)$ as a functional of u(z). Requiring that this functional satisfy (7) will then give us the integral equation for u(z), from which the flux $\int u(z)dz$ is determined.

We now consider the boundary conditions. If a fraction ε of the quasiparticles incident at a wall are specularly reflected, then the distribution function at the lower wall obeys

$$n_{\vec{p}}\left(-\frac{D}{2}\right) = (1 - \varepsilon)n_{\vec{p}}^0 + \varepsilon n_{\vec{p}^*}\left(-\frac{D}{2}\right), \quad p_z > 0 \tag{13}$$

where $\vec{p}^* = (p_x, p_y, -p_z)$. At the upper wall the distribution function obeys

$$n_{\vec{p}}\left(\frac{D}{2}\right) = (1 - \varepsilon)n_{\vec{p}}^0 + \varepsilon n_{\vec{p}^*}\left(\frac{D}{2}\right), \quad p_z > 0 \tag{14}$$

since $n_{\vec{p}}^0$ is independent of the sign of p_z. To express these conditions in terms of the deviation from local equilibrium, we go back to the definition (5) of the local equilibrium distribution function and expand to linear order in the perturbation F:

$$n_{\vec{p}}^{le}\left(-\frac{D}{2}\right) \cong n_{\vec{p}}^0 + \left(\frac{\partial n_p^0}{\partial \varepsilon_p}\right)\left\{\sum_{\vec{p}}, f_{\vec{p}\vec{p}}, \delta n_{\vec{p}}, \left(-\frac{D}{2}\right) - p_x u\left(-\frac{D}{2}\right)\right\} \quad . \tag{15}$$

Substituting $n_{\vec{p}}\left(-\frac{D}{2}\right) = n_{\vec{p}}^{le}\left(-\frac{D}{2}\right) + \delta\vec{n}_{\vec{p}}\left(-\frac{D}{2}\right)$ into (13) and using (15), we find

$$\delta\bar{n}_{\vec{p}}(z) - \varepsilon\delta\bar{n}_{\vec{p}*}(z) = \left(\frac{\partial n^0_p}{\partial\varepsilon_p}\right)\left\{(1-\varepsilon)p_x u\left(-\frac{D}{2}\right) + \varepsilon\sum_{\vec{p}'} f_{\vec{p}*\vec{p}'}\,\delta n_{\vec{p}'}\left(-\frac{D}{2}\right)\right.$$

$$\left. - \sum_{\vec{p}'} f_{\vec{p}\vec{p}'}\,\delta n_{\vec{p}'}\left(-\frac{D}{2}\right)\right\} \quad . \tag{16}$$

Consider the Fermi liquid interaction terms in (16). Although they are formally of the same order as the other terms, our model of what happens at the boundaries is sufficiently crude that we can probably omit them without making the description any less accurate. Recall that ε is a phenomenological parameter that reflects the degree of correlation between incident and reflected quasiparticles. We assume that the effect of the interaction terms in (16) may be adequately approximated by choosing a different value of ε than we would have done had no interactions been present. Even without this assumption we have no way of calculating ε for the surfaces of interest, and retaining the interaction term would make the calculation much more difficult. Thus (16) becomes

$$\delta\bar{n}_{\vec{p}}\left(-\frac{D}{2}\right) - \varepsilon\delta\bar{n}_{\vec{p}*}\left(-\frac{D}{2}\right) = \left(\frac{\partial n^0_p}{\partial\varepsilon_p}\right)(1-\varepsilon)p_x u\left(-\frac{D}{2}\right), \qquad p_z > 0 \quad . \tag{17}$$

The analogous equation for the other boundary is

$$\delta\bar{n}_{\vec{p}}\left(\frac{D}{2}\right) - \varepsilon\delta\bar{n}_{\vec{p}}\left(\frac{D}{2}\right) = \left(\frac{\partial n^0_p}{\partial\varepsilon_p}\right)(1-\varepsilon)p_x u\left(\frac{D}{2}\right) \quad . \tag{18}$$

To apply these conditions, we go back to the general solution (12) of the transport equation and evaluate it a $z = -\frac{1}{2}D$ and $z = +\frac{1}{2}D$, substituting these results into (17) and (18) respectively. This gives us two equations for the two unknowns $A_{\vec{p}}$ and $A_{\vec{p}*}$. Putting the solution for $A_{\vec{p}}$ into (12) gives us $\delta\bar{n}_{\vec{p}}(z)$ for $p_z > 0$: the solution for $p_z < 0$ is found by exploiting the

mirror symmetry of the problem:

$$\delta\vec{n}_{\vec{p}}(z) = \delta\vec{n}_{\vec{p}^*}(-z)$$

and

$$u(z) = u(-z) \quad .$$

When we follow this procedure, the results are

$$\delta\vec{n}_{\vec{p}}(z) = e^{-m^*z/p_z\tau}\left\{\frac{-(1-\varepsilon)u\left(\frac{D}{2}\right)}{\varepsilon\exp(-m^*D/2p_z\tau)-\exp(m^*D/2p_z\tau)} - \frac{\varepsilon\exp(-m^*D/2p_z\tau)}{\varepsilon\exp(-m^*D/2p_z\tau)-\exp(m^*D/2p_z\tau)}\right.$$
$$\left.\int_{-D/2}^{D/2} dz'\exp(m^*z'/p_z\tau)\left(\frac{\partial u}{\partial z},-\frac{F}{p_z}\right)+\int_{-D/2}^{z} dz'\exp(m^*z'/p_z\tau)\left(\frac{\partial u}{\partial z},-\frac{F}{p_z}\right)\right\}p_x\left(\frac{\partial n_p^0}{\partial\varepsilon_p}\right), \quad p_z > 0 \tag{21a}$$

$$\delta\vec{n}_{\vec{p}}(z) = e^{-m^*z/p_z\tau}\left\{\frac{-(1-\varepsilon)u\left(\frac{D}{2}\right)}{\varepsilon\exp(m^*D/2p_z\tau)-\exp(-m^*D/2p_z\tau)} + \frac{\exp(-m^*D/2p_z\tau)}{\varepsilon\exp(m^*D/2p_z\tau)-\exp(-m^*D/2p_z\tau)}\right.$$
$$\left.\int_{-D/2}^{D/2} dz'\exp(m^*z'/p_z\tau)\left(\frac{\partial u}{\partial z},-\frac{F}{p_z}\right)+\int_{-D/2}^{z} dz'\exp(m^*z'/p_z\tau)\left(\frac{\partial u}{\partial z},-\frac{F}{p_z}\right)\right\}p_x\left(\frac{\partial n_p^0}{\partial\varepsilon_p}\right), \quad p_z < 0 \ . \tag{21b}$$

It will be noted that the distribution function is discontinuous at $p_z = 0$. This is because the particles which have just been scattered by a wall have a substantially different distribution than those about to be scattered due to the large change in momentum that occurs in scattering.

We can now impose the condition (7) that the average of the momentum over the deviation from local equilibrium vanishes. The only component that does not vanish trivially is the x-component, thus the equation of interest is

$$0 = \int d^3p \; p_x \; \delta\vec{n}_{\vec{p}}(z) \quad . \tag{22}$$

Inspection of (21a) and (21b) shows that $(\partial n_p^0/\partial \varepsilon_p)$ is the only factor in $\delta\bar{n}_{\vec{p}}(z)$ that varies rapidly as a function of $|\vec{p}|$ near p_F. Thus, as long as $T \ll T_F$, we may replace it by $-\delta(\varepsilon_p - \varepsilon_F)$. When we integrate using spherical coordinates in (22), the effect of this δ-function is to set $|p| = p_F$ everywhere. The φ-integral is trivial, so that, defining $\mu = \cos\theta$ and the mean free path $\ell = p_F\tau/m^*$, (22) becomes

$$0 = \int_0^1 d\mu\,(1-\mu^2)e^{-z/\ell\mu}\left\{\frac{-(1-\varepsilon)u\left(\frac{D}{2}\right)}{\varepsilon\exp(-D/2\ell\mu)-\exp(D/2\ell\mu)} - \frac{\varepsilon e^{-D/2\ell\mu}}{\varepsilon\exp(-D/2\ell\mu)-\exp(D/2\ell\mu)}\right.$$
$$\left.\int_{-D/2}^{D/2} dz'\exp(z'/\ell\mu)\left(\frac{\partial u}{\partial z'} - \frac{F}{p_z}\right) + \int_{-D/2}^{z} dz'\exp(z'/\ell\mu)\left(\frac{\partial u}{\partial z'} - \frac{F}{p_z}\right)\right\}$$
$$+ \int_{-1}^{0} d\mu\,(1-\mu^2)\exp(-z/\ell\mu)\left\{\frac{-(1-\varepsilon)u\left(\frac{D}{2}\right)}{\varepsilon\exp(D/2\ell\mu)-\exp(D/2\ell\mu)} + \frac{\exp(-D/2\ell\mu)}{\varepsilon\exp(D/2\ell\mu)-\exp(-D/2\ell\mu)}\right.$$
$$\left.\int_{-D/2}^{D/2} dz'\exp(z'/\ell\mu)\left(\frac{\partial u}{\partial z'} - \frac{F}{p_z}\right) + \int_{-D/2}^{z} dz'\exp(z'/\ell\mu)\left(\frac{\partial u}{\partial z'} - \frac{F}{p_z}\right)\right\} . \qquad (23)$$

We next integrate by parts wherever $\partial u/\partial z'$ appears. It is found after some algebra that the surface terms from these integrations cancel the terms in (23) containing $u(D/2)$. If we define a dimensionless velocity

$$U(z) = \frac{m^* u(z)}{F\tau}$$

and divide by $-F\tau/m^*$ we have

$$0 = \int_0^1 d\mu\,(1-\mu^2)\left\{-2U(z) - \frac{\varepsilon\exp(-z/\ell\mu)\exp(-D/2\ell\mu)}{\varepsilon\exp(-D/2\ell\mu)-\exp(D/2\ell\mu)}\ \frac{1}{\ell\mu}\int_{-D/2}^{D/2} dz'\exp(z'/\ell\mu)(1+U(z'))\right.$$
$$\left. - \frac{\exp(z/\ell\mu)\exp(D/2\ell\mu)}{\varepsilon\exp(-D/2\ell\mu)-\exp(D/2\ell\mu)}\ \frac{1}{\ell\mu}\int_{-D/2}^{D/2} dz'\exp(z'/\ell\mu)(1+U/z'))\right.$$

$$+\frac{\exp(-z'/\lambda_\mu)}{\lambda_\mu}\int_{-D/2}^{z}dz'\exp(z'/\lambda_\mu)(1+U(z'))+\frac{\exp(z'/\lambda_\mu)}{\lambda_\mu}\int_{-D/2}^{-z}dz'\exp(z'/\lambda_\mu)(1+U(z'))\Big\}\ . \tag{24}$$

Further manipulations permit us to cast this in the form

$$U(z)=\frac{3}{4\ell}\int_0^1 d\mu\,(\frac{1}{\mu}-\mu)\frac{1}{1-\varepsilon\exp(-D/\lambda_\mu)}\Big\{\exp(-z/\lambda_\mu)\Big[\int_{-D/2}^{z}dz'\exp(z'/\lambda_\mu)(1+U(z'))-\varepsilon\exp(-D/\lambda_\mu)$$

$$\int_{D/2}^{z}dz'\exp(z'/\lambda_\mu)(1+U(z'))\Big]+\exp(z/\lambda_\mu)\Big[\int_{-D/2}^{-z}dz'\exp(z'/\lambda_\mu)(1+U(z'))-\varepsilon\exp(-D/\lambda_\mu)$$

$$\int_{D/2}^{-z}dz'\exp(z'/\lambda_\mu)(1+U(z'))\Big]\Big\}\ . \tag{25}$$

We now define the Knudsen[9] number (ratio of cell thickness to mean free path)

$$\kappa=\frac{D}{\ell}=\frac{m^*D}{p_F}\ , \tag{26}$$

a dimensionless coordinate $\zeta = z/D$, and redefine the functional dependence of the dimensionless velocity U so that $U(z) \to U(\zeta)$. With a few more steps we obtain

$$U(\zeta)=\frac{3}{4}\kappa(1+\varepsilon)\int_0^1 d\mu\,(\frac{1}{\mu}-\mu)\,\frac{1}{1-\varepsilon\exp(-\kappa/\mu)}\int_{-\frac{1}{2}}^{\frac{1}{2}}d\zeta'\exp(-\kappa|\zeta-\zeta'|/\mu)(1+U(\zeta')) \tag{27}$$

This is the integral equation for the velocity profile.

IV. Solution for Flow Rate

We have solved this equation numerically by doing a Gaussian integration[10] on μ, using a finite element method to convert the integral equation into a matrix equation, and then using an iterative technique. This gives a discretized representation for the solution $U(\zeta)$ which we integrate numerically across the cell. We then have the quantity

$$\int_{-\frac{1}{2}}^{\frac{1}{2}}U(\zeta)d\zeta=\langle U\rangle=\frac{m^*\langle u\rangle}{F\tau}=\kappa\frac{p_F\langle u\rangle}{FD} \tag{28}$$

as a function of $\varkappa$ and ε. In order to see the $\varkappa$-dependence of $\langle u \rangle$ more clearly, we divide (28) by $\varkappa$ and plot the result for several values of ε in fig. 2.

The resulting curves have several striking features. For $\varkappa \geq 3$ the various values of ε give a family of straight lines whose slope with respect to $\varkappa$ is close to the ratio 5/12. We shall see that this is the exact value required to recover classical bulk fluid behavior in the limit of large $\varkappa$: one can also verify analytically that the solution of the integral equation (27) has just this behavior. Thus, the only manifestation of a finite size effect for $\varkappa \geq 3$ is the $\varkappa$-independent offset of these lines.[11]

At small $\varkappa$ the quantity $\langle U \rangle / \varkappa$ diverges logarithmically. This divergence arises from the rather artificial assumption that quasiparticles scattered almost parallel to the wall move slowly away from it and do not interact with it any more. These particles will take longer than most others to cross the cell, and hence will be acted upon by the driving field for a long time, giving a large contribution to the total current; however, these particles are the ones most likely to scatter against other particles before reaching the other side. A logarithmic divergence of $\langle U \rangle / \varkappa$ with $\varkappa$ can be shown to result from this situation. In a real cell, in which quasiparticles reflected parallel to a wall will be re-scattered by surface inhomogeneities, we expect a large but finite flux at $\varkappa = 0$. Suppose the inhomogeneities in the surface have typically an amplitude α and a wavelength L. Then the minimum possible angle between the wall and the momentum of a quasiparticle traveling away from the wall is approximately α/L. The quantity $\langle U \rangle / \varkappa$ will cease going as $-\ln \varkappa$ when $\varkappa \cong \alpha/L$; instead, we expect it to go to a constant value of roughly $\ln(L/\alpha)$.

In the intermediate $\varkappa$ region we find that $\langle U \rangle / \varkappa$ goes through a minimum in the vicinity of $\varkappa = \frac{1}{2}$, and then approaches the linear behavior seen at large $\varkappa$. If we extrapolate the high-$\varkappa$ behavior down into the intermediate region,

and find the difference between this linear function and the actual $\langle U \rangle / \kappa$, we obtain a measure of the deviation from linear behavior. This deviation, which we call δ, is displayed in Table 1; it is seen to drop off rapidly as κ increases.

The ε-dependence of the results is also worthy of note. It can be well approximated by an additive term independent of κ. This implies that our choice of ε will not affect the qualitative structure of the results. We note that a very similar result has been found for the case of classical rarified gas dynamics[12].

The flow rate $\langle u \rangle$ through the cell determines the rate at which the applied force F does work on the system; this dissipation is what will usually be measured in an experiment. One way to characterize the finite size effect is to say that the fluid behaves as if it had a different viscosity than would an infinite sample of the same fluid. We define this "effective viscosity" to be that which would give the correct flux (or dissipation) of the actual cell when substituted into the equations of hydrodynamics. In the classical theory the flux is

$$\langle u \rangle = \frac{D^2 F n}{12 \eta} \tag{29}$$

where n is the number density in the fluid. For the finite cell we define

$$\eta_{ff} = \frac{D^2 F n}{12 \langle u \rangle} \tag{30}$$

We now divide both sides by the viscosity of the bulk fluid, using (28) and the relation

$$\eta_{Bulk} = \frac{1}{5} p_F v_F n \tau \ , \tag{31}$$

and obtain

$$\frac{\eta_{eff}}{\eta_{Bulk}} = \frac{5}{12} \frac{\kappa^2}{\langle U \rangle} \tag{32}$$

This ratio must obviously approach unity at large κ: the asymptotic behavior mentioned above for the ratio $\langle U \rangle / \kappa$ clearly insures that this will be the case. The quantity (32) is plotted in fig. 3 as a function of κ for several values of ε.

V. Application to Experiments

These results have been applied to the interpretation of some experiments performed by Parpia[1,3] and Archie[2]. In these experiments, a disc-shaped cavity in an epoxy cell is filled with ^{3}He and caused to vibrate torsionally about its central axis. The drive voltage which is required to maintain constant amplitude with changing temperature is then measured. The measured voltage is proportional to the total rate of energy dissipation in the cell, which is the sum of the dissipation in the liquid and a "nuisance damping" associated only with the apparatus.

Some results of these experiments are given in fig. 1 of reference 1. The effective viscosity, obtained from the driving voltage required to maintain constant amplitude, is plotted as a function of T^2; it is linear above about $T = 3.5$ mK , and shows an upward curvature from this temperature down to the transition temperature (below which it jumps sharply upward.) The present calculation was originally undertaken in the hope of understanding this curvature.

To apply the results of the previous section of this paper, we make several observations: (i) the frequency in these experiments is less than 1 KHz, permitting a steady-state analysis, (ii) the cavity radius is about forty times its thickness, permitting an element of the cell to be treated as an element of an infinite slab executing translational vibrations with an amplitude of $r\theta_0$, where r is the distance of the actual element under consideration from the axis of the cell, and θ_o is the amplitude of the torsional vibration, (iii) Edge effects may also be neglected, (iv) the vibrational amplitude is very small in these experiments (less than 10^{-6} radians) so that a linearized theory is well justified.

It is easy to relate our parameter $\varkappa$ to the temperature. We have $\varkappa = D/\lambda = D/v_F\tau$, and in the normal phase the relaxation time is inversely proportional to the square of the temperature.[5] Writing

$$\tau = AT^{-2} , \tag{33}$$

we have

$$\varkappa = \frac{DT^2}{v_F A} . \tag{34}$$

Since v_F and A depend only on the pressure, we see that the Knudsen number is proportional to the square of the temperature for constant D. The constant of proportionality is found from experimental data; see Table 2.

We must now relate the dissipation to the dimensionless flow rate found in the previous section. In the frame of reference of the wall, there is a fictitious force of -ma per particle, where a is the instantaneous acceleration of the wall in the laboratory frame. We use our static theory to obtain the response to this force; the relative error involved in doing this will be of order $\omega\tau \cong 10^{-3}$ in our case. The dissipation in an element dA of the cell is

$$d\dot{E} = -nma\langle u\rangle DdA = \frac{n(ma)^2}{p_F} \frac{\langle U\rangle}{\varkappa} D^2 dA \tag{35}$$

Now we replace the square of the acceleration by its time average over a complete cycle of the motion:

$$\langle a^2\rangle_{time} = \langle (\theta_0 r\omega^2 \cos\omega t)^2\rangle_{time} = \frac{\theta_0^2 r^2 \omega^4}{2} \tag{36}$$

We note that the dissipation, being proportional to the entropy production, must be frame-independent, so that the value calculated in the instantaneous reference frame of the wall may be taken over to the laboratory frame without

change. Using (35) and (36), and integrating over the area of the entire cell, we get

$$\dot{E} = \frac{D^2 m^2 n \theta_0^2 \omega^4}{2p_F} \frac{\langle U \rangle}{\varkappa} 2\pi \int_0^R r^3 dr \tag{37}$$

where R is the radius of the cell; we then have

$$\dot{E} = \frac{\pi}{4} \frac{D^2 m^2 n}{p_F} \theta_0^2 \omega^4 R^4 \frac{\langle U \rangle}{\varkappa} = \frac{1}{64\pi} \frac{M^2 \theta_0^2 \omega^4}{n p_F} \frac{\langle U \rangle}{\varkappa} \tag{38}$$

where M is the total mass of the fluid in the cell.

This relation connects the function $\langle U \rangle / \varkappa$ which was calculated in section III and plotted in fig. 2 with the dissipation in the disc of fluid, the latter being proportional to the drive voltage, modulo a constant. The proportionality of $\langle U \rangle / \varkappa$ to this voltage enables us to see what the theory implies about the experiments. For purposes of comparison let us define $\varkappa_{\frac{1}{2}}$ as that value of $\varkappa$ for which the derivative of $\langle U \rangle / \varkappa$ with respect to $\varkappa$ has half of its large-$\varkappa$ asymptotic value. Similarly we define $T^2_{\frac{1}{2}}$ as that value of T^2 for which the derivative of the drive voltage with respect to T^2 has half of its limiting value. By expressing this $T^2_{\frac{1}{2}}$ as a Knudsen number, we can determine whether the curvature in the experimental plot falls in the right temperature range to be the mean free path-finite size effect.

In fact it does not. We find that $\varkappa_{\frac{1}{2}} \cong 1$ for all values of ε. On the other hand the temperature $T_{\frac{1}{2}}$ corresponds to values of $\varkappa \cong 36$ for p = 29 bar and $\varkappa \cong 7$ for p = 0. Furthermore, we see from Table 2 that for a cell of the size used at Cornell, the curvature predicted by the theory should only be seen at pressures of a few bar, but the experimental curvature is seen at high pressures as well. We conclude that the curvature in the drive vs. T^2 plot is <u>not</u> due to the mean free path effect explored in this paper, and its explanation

must be sought elsewhere, perhaps in the thermometry; the effect calculated here is being masked by this other, unknown effect.

There are three courses of action that might be followed to actually see the mean free path effect. (i) Identify the cause of the curvature in the experimental plot, and remove it; this should unmask the upward curvature due to the mean free path effect, which should be noticeable at low pressures. (ii) Remove the nuisance damping, so that the ε-dependent vertical translation of the curves in fig. 2 can be determined experimentally; this part of the effect is significant even when the curvature is too small to be seen. (iii) Repeat the experiment in a thinner cell, so that a given value of κ will correspond to a higher temperature.

Finally, we note that in the superfluid phases the mean free path is expected to become very large[4], so that almost all experimental cells will have dimensions of similar or smaller magnitude. The calculation given here applies only to the normal phase, but the method should be readily extensible at least to the B-phase.[14] We hope to treat this problem in a future publication.

AKNOWLEDGEMENTS

The author gratefully acknowledges useful discussions with N.W. Ashcroft, Hassan Aref, J.W. Wilkins, C. Archie, J. Parpia and J.D. Reppy.

This work was supported in part by the National Aeronautics and Space Administration through grant no. NGR-33-010-188 and the National Science Foundation through grant no. DMR-77-18329.

Table 1

$\varkappa$	δ
0.2	.5869
0.4	.3401
0.6	.2266
0.8	.1609
1.0	.1176
1.2	.0868
1.4	.0638
1.6	.0469
1.8	.0330
2.0	.0225

Deviation δ of the function $\langle U \rangle / \varkappa$ from its linear behavior at high $\varkappa$.

Table 2

p, bar	T_c, mK	λ, μm	$\varkappa$, D=95μm	$\varkappa$, D=20μm	δ
0	1.0	68.0	1.40	0.295	.4434
3	1.4	29.2	3.25	0.684	.1959
6	1.6	19.5	4.87	1.03	.1126
12	2.08	9.36	10.1	2.13	.0174
18	2.31	6.26	15.2	3.20	
24	2.45	4.65	20.4	4.29	
30	2.56	3.64	26.1	5.49	

The mean free path and Knudsen number evaluated at the transition temperature for several pressures, and for two cell thickness. We have used data from Wheatley.[13] In the last columm, the deviation δ is evaluated at the transition temperature, for a cell width of 20 μm. It is negligible at pressures above about 12 bar.

REFERENCES

1. J.M. Parpia, D.J. Sandiford, J.E. Berthold, and J.D. Reppy, Phys. Rev. Lett. 40, 565 (1978).
2. C.N. Archie, 1979, Thesis, Cornell University, unpublished.
3. J.M. Parpia, 1979, Thesis, Cornell University, unpublished.
4. Y.A. Ono, in Physics at Ultralow Temperatures, Proceedings of the Hakone International Symposium, 1977, T. Sugawara, ed. Phys. Soc. Japan, Tokyo 1978.
5. G. Baym and C.J. Pethick, "Landau Fermi Liquid Theory and Low Temperature Properties of Liquid ^{3}He" in Physics of Liquid and Solid Helium, K.H. Benneman and J.B. Ketterson, eds., Wiley, New York, 1976.
6. In comparing theory to experiment we use the "viscous relaxation time" τ_η so as to insure that the high-$\varkappa$ limit gives the correct viscosity.
7. K. Fuchs, Proc. Cambridge Phil. Soc. 34, 100
8. It can be shown that to linear order in F there is no change in the chemical potential. The reason is that the chemical potential can vary only in the z-direction, but the applied force is in the x-direction. The dissipation in the fluid will give rise to temperature gradients, but we expect these to be small because of the very high thermal conductivity of ^{3}He.
9. M. Knudsen, Kinetic Theory of Gases, Methuen, London 1950.
10. M. Abramowitz and I.A. Stegun, Handbook of Mathematical Functions, Dover, New York, 1970.
11. One can also show analytically that for $\varepsilon = 0$ the high temperature asymptote intercepts the vertical axis at $\langle U\rangle/\varkappa = 15/8$.
12. C. Cerignani, in Rarified Gas Dynamics, Proceedings of the 3rd International Symposium, Vol. II ed. J.A. Larmann p. 92. Academic Press, New York 1963. C. Cerignani and C.D. Pagani, in Rarified Gas Dynamics, Proceedings of

the 6th International Symposium, Vol. I, eds. L. Trilling and H.Y. Wachman, Academic Press, New York 1969.

M.N. Kogan, Rarified Gas Dynamics Plenum, New York 1969, section 4.3.

13. J. Wheatley, Rev. Mod. Phys. 47, 415 (1975).

14. A.J. Leggett, Rev. Mod. Phys. 47, 331 (1975).

Figure Captions

Figure 1 Sketch of the idealized viscometer cell, showing an example of the velocity profiles found in the calculation. The curves represent $u_x(z)$ for $\varkappa = 3$ and $\varepsilon = 0$, 0.2, 0.4 and 0.6; each mark on the horizontal axis represents $5F\tau/m^*$.

Figure 2 The quantity $\langle U\rangle/\varkappa$ as a function of $\varkappa$ for several values of ε. We have $\langle U\rangle/\varkappa = p_F\langle u\rangle/FD$ where $\langle u\rangle$ is the flow velocity averaged across the cell, F is the driving force per particle, D is the cell width, and p_F is the Fermi momentum.

Figure 3 The ratio of the "effective viscosity" to the true shear viscosity of a bulk sample of the fluid, as a function of $\varkappa$, for several values of ε.

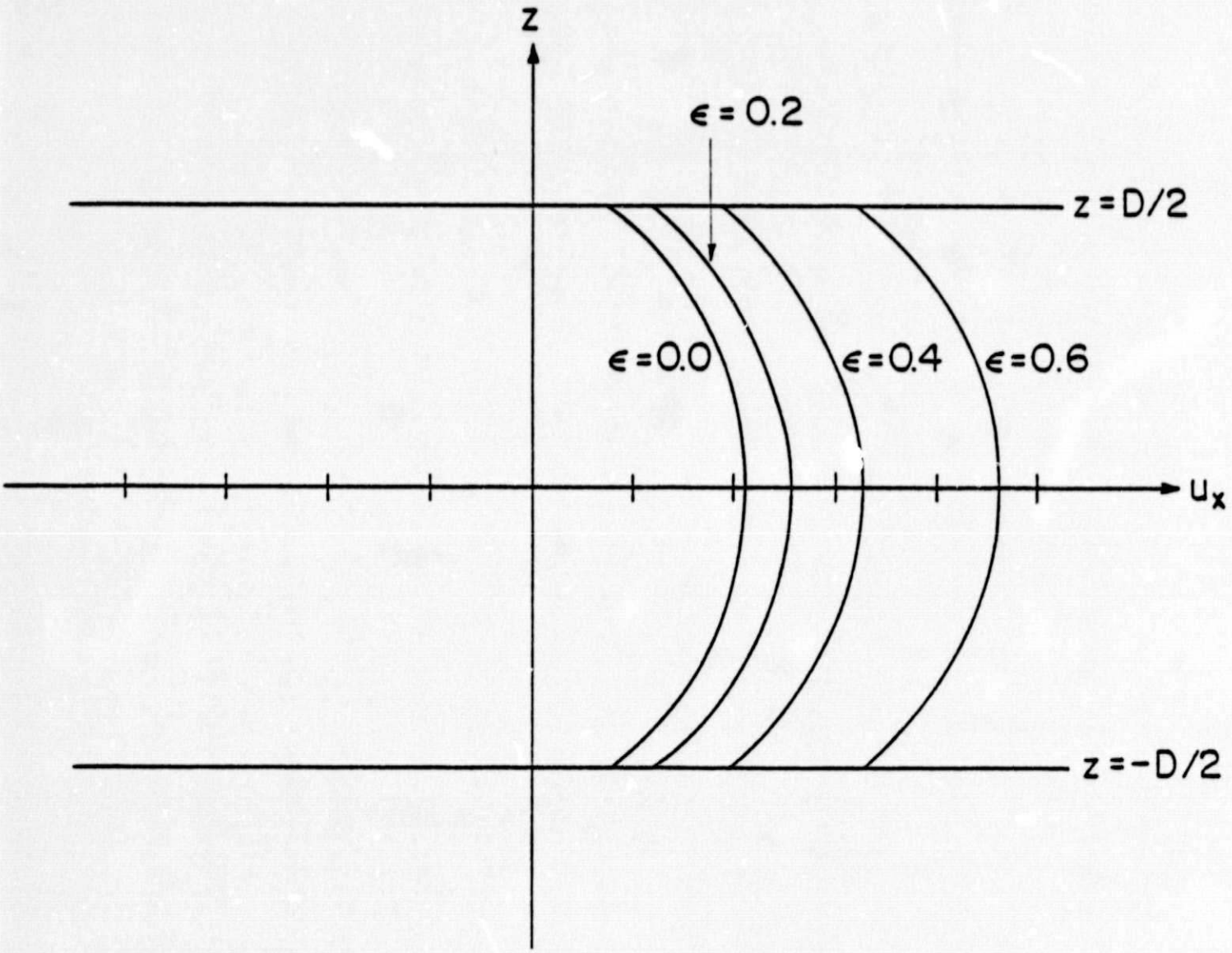

Figure 1

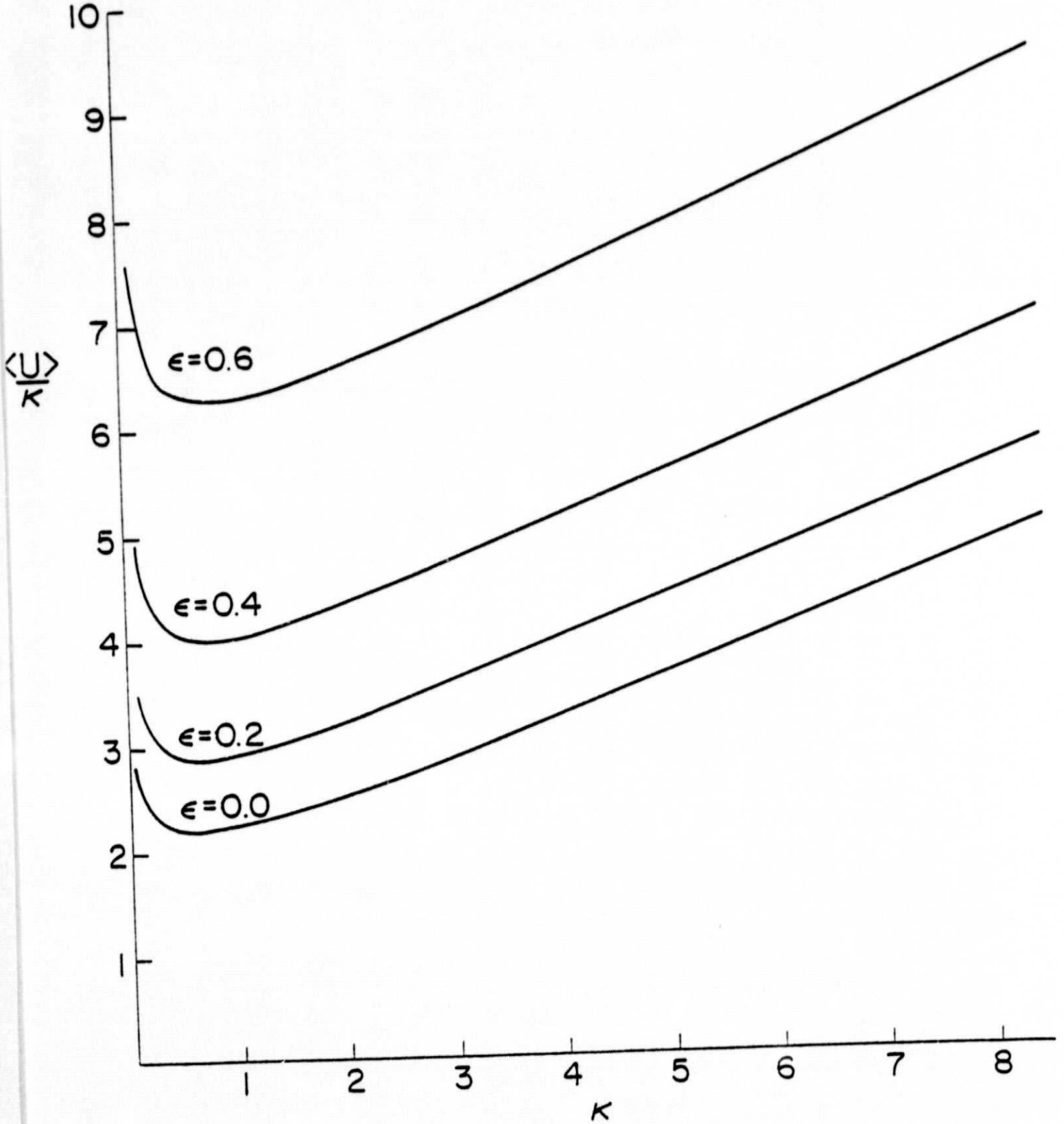
10
9
8
7
6
5
4
3
2
1
$\frac{\langle U \rangle}{K}$
ϵ=0.6
ϵ=0.4
ϵ=0.2
ϵ=0.0
1
2
3
4
5
6
7
8
K

Figure 2

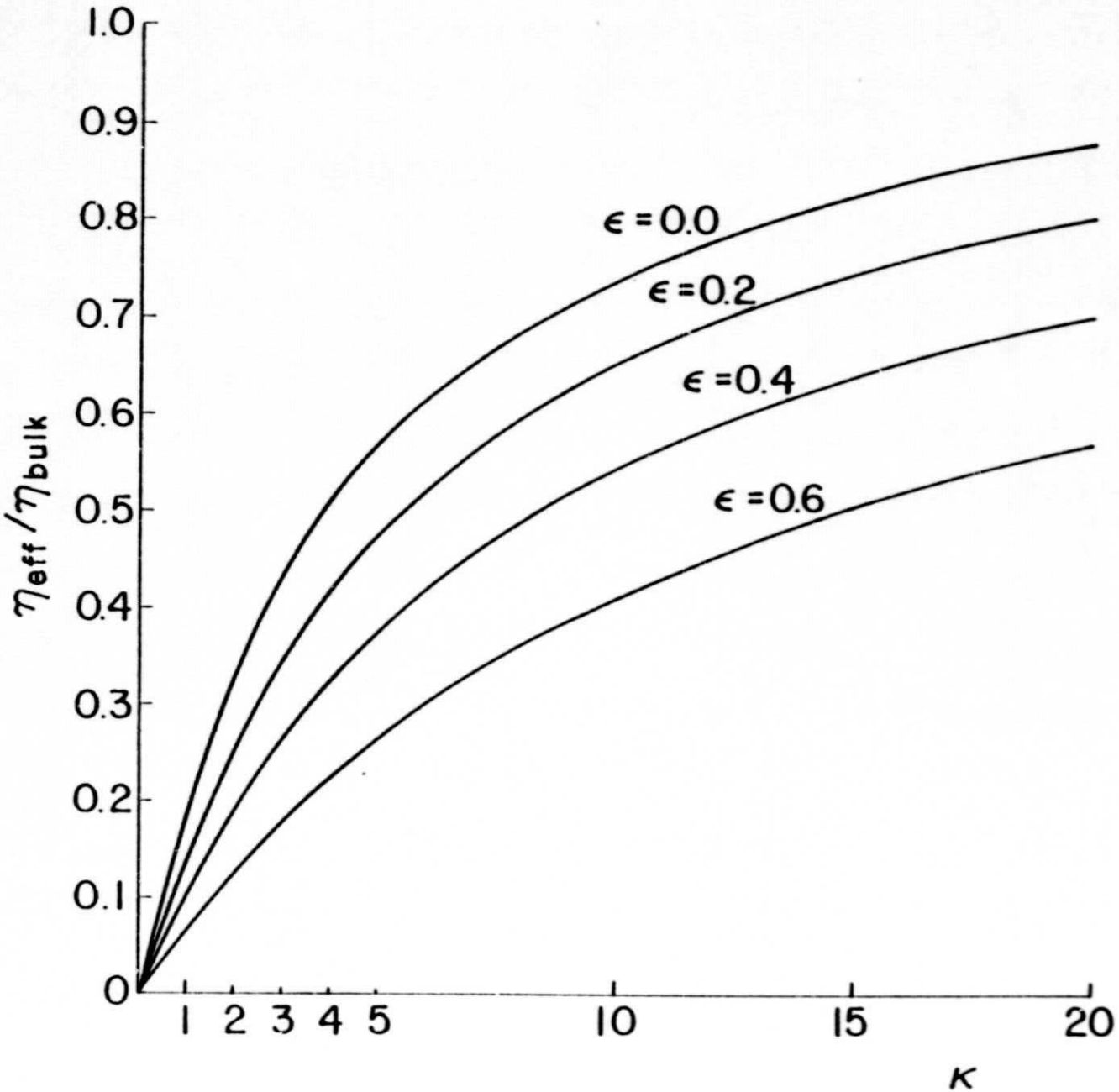
1.0
0.9
0.8
0.7
0.6
0.5
0.4
0.3
0.2
0.1
0
η_{eff}/η_{bulk}
$\epsilon = 0.0$
$\epsilon = 0.2$
$\epsilon = 0.4$
$\epsilon = 0.6$
1 2 3 4 5
10
15
20
κ

Figure 3